

Pile groups under axial loading: an appraisal of simplified nonlinear prediction models

Brian B. Sheil^{1*}, Bryan A. McCabe², Emilios M. Comodromos³, Barry M. Lehane⁴

¹Departmental Lecturer, Department of Engineering Science, University of Oxford, U.K.

²Senior Lecturer, Civil Engineering, College of Engineering and Informatics, National University of Ireland, Galway, Ireland

³Professor, Department of Civil Engineering, University of Thessaly, Greece.

⁴Professor, School of Civil, Environmental and Mining Engineering, The University of Western Australia, Crawley, Australia

*Corresponding author. Email: brian.sheil@eng.ox.ac.uk. Tel.: +44 (0)1865 2 83148

1 **ABSTRACT**

2 The settlement behaviour of vertically-loaded pile groups has been the subject of an extensive
3 body of research over the past two decades. In particular, this work has identified the over-
4 conservatism associated with predictions of pile interaction derived from elastic theory and the
5 corresponding amplification of group settlement relative to single pile values. Researchers have
6 since redoubled efforts to refine settlement predictions for pile groups towards more
7 economical design, largely through more rigorous treatment of soil stiffness nonlinearity.
8 Although foundation design engineers are increasingly employing three-dimensional
9 continuum analyses to quantify pile interaction on a site-specific basis, simplified design
10 approaches remain an integral part of preliminary foundation design. The purpose of this paper
11 is to undertake a critical examination of these methods with a view to increasing their potential
12 for take-up by foundation engineering practitioners. A database of simplified models has been
13 collated for the prediction of nonlinear pile interaction that exists within vertically-loaded pile
14 groups. These models are categorised as either analytical or empirical. The development,
15 limitations, and range of applicability of these models are explored in detail in the context of
16 some published case histories.

17 INTRODUCTION

18 Pile foundations have been used for centuries as a means of transmitting structural loads to
19 competent strata at depth in the ground. Piles installed in groups have the potential to carry
20 large loads and are often the only viable solution when structures to be supported are heavy, or
21 when the ground conditions are challenging. Traditionally, the emphasis in pile design was on
22 predicting ultimate pile capacity, with a large factor of safety ensuring that settlements were
23 small, formal estimates of which could often be avoided. More recently, this focus has shifted
24 towards more economical serviceability limit-state design thereby prompting considerable
25 research effort to refine predictions of single pile and pile group settlement. In particular, this
26 has necessitated more reliable modelling of the development of pile-soil interface resistance
27 during loading as well as more realistic treatment of pile-to-pile interaction.

28 An important outcome of research into the settlement behaviour of pile groups under axial
29 loads is that predictions based on elastic theory alone are excessively conservative. As a result,
30 the application of nonlinear frameworks to pile groups has increased substantially over the last
31 two decades. Within a nonlinear framework, pile settlement is no longer uncoupled from the
32 ultimate capacity and therefore an accurate estimation of capacity is a prerequisite for a
33 rigorous analysis of the serviceability limit state. While three-dimensional nonlinear
34 continuum analyses are becoming more commonplace, simplified design approaches remain
35 an integral part of preliminary foundation design. There is now a myriad of approaches in the
36 literature for the prediction of nonlinear pile interaction. The purpose of this paper is to
37 undertake a critical examination of a selection of these methods, in the context of selected case
38 histories, with a view to increasing their potential for take-up by foundation engineering
39 practitioners; the primary focus is on developments since the seminal review paper on pile
40 groups by Poulos (2006).

41 The settlement behaviour of piled foundations subjected to vertical loads is potentially
42 governed by both pile-to-pile interaction and pile-soil-raft interaction (Ghalesari et al. 2015).
43 Pile interaction effects, in particular those that exist between pile shafts, necessitate rigorous
44 treatment as settlements are amplified relative to single pile values. Interaction between pile
45 shafts is therefore central to this review. The role of soil stiffness nonlinearity on pile
46 interaction is first considered. A database of existing simplified nonlinear models is collated,
47 and categorised as either empirical or analytical. The associated assumptions, limitations, and
48 applicability of each model are also discussed. Clearly the accuracy of any predictive model is
49 dependent on the appropriateness of the input parameters. In light of this, careful consideration

50 of the pile type, installation effects, and the corresponding soil responses (dilation, pore
51 pressure generation and evolution of stresses for example) is paramount.

52

53 **BACKGROUND: PILE GROUP INTERACTIONS**

54 *Pile-soil-raft interaction*

55 According to Comodromos et al. (2016), the resistance of a piled raft can be partitioned into
56 three stages depending on the group settlement normalized by the pile diameter, S_{ng} :

- 57 1. $0\% < S_{ng} < 1.5\%$: the resistance of both the piles and the raft are linear and the resistance
58 contribution from the raft is insignificant and therefore commonly ignored (Mandolini
59 and Viggiani 1997; Xu and Zhang 2007; Kumar et al. 2017);
- 60 2. $1.5\% < S_{ng} < 4\%$: the piles exhibit up to ~90% of their limit capacity;
- 61 3. $S_{ng} > 4\%$: additional resistance of the piled raft is essentially attributed to the raft.

62 Those authors reported that the maximum contribution from the raft (acting within the piled
63 raft system) was considerably lower than the corresponding resistance of an isolated raft. It was
64 also noted that the maximum resistance provided by the piles was essentially unaffected by the
65 existence of the raft (Comodromos et al. 2009). In light of this, the spring elements replacing
66 the soil resistance around the piles may be considered independent from those simulating the
67 resistance under the raft.

68

69 *Nonlinear two-pile interaction factors*

70 The interaction factor method (IFM) is the most common means of accounting for pile
71 interaction in the design of pile groups. This process essentially applies an amplification factor
72 to the settlement of a single pile with the same applied load at the pile head. Initially, the
73 interaction between a pair of piles (i and j) is quantified as a ‘two-pile interaction factor’, α :

$$74 \quad \alpha = \frac{\text{Additional settlement of pile } j \text{ due to nearby loaded pile } i}{\text{Settlement of single pile under its own (equivalent) load}} \quad (1)$$

75 Values of α may be computed for each pile spacing, s , occurring within the group. The principle
76 of superposition is then applied to calculate the cumulative interaction occurring within the
77 group. However, inconsistencies in how α is calculated feature in the literature. The receiver
78 pile may be load-free (henceforth referred to as ‘Approach I’; see Fig. 1(a)) or loaded
79 (henceforth referred to as ‘Approach II’, see Fig. 1(b)). When used within a linear elastic (LE)

80 framework, both approaches yield the same result. For real soils, however, the increased level
81 of shear strain in the vicinity of a loaded pile causes a corresponding reduction in the soil
82 modulus. The consideration of soil nonlinearity therefore results in different values of α
83 depending on the applied load level and whether Approach I or Approach II is adopted
84 (McCabe and Sheil 2015).

85

86 *Validity of superimposing nonlinear interaction factors – numerical investigations*

87 The principle of superposition is not valid in nonlinear engineering problems. Nevertheless, a
88 number of studies have investigated the role of soil stiffness nonlinearity in pile interaction and
89 pile group settlement. Caputo and Viggiani (1984) described a case history on the interaction
90 between an identical pile pair. The pile load tests consisted of one loaded pile while the other
91 nearby pile remained load-free (i.e. Approach I). These authors noted that while the response
92 of the loaded pile was highly nonlinear, the settlement of the load-free pile increased linearly
93 with increasing applied load on the loaded pile (see Fig. 2).

94 Using three-dimensional finite element analysis (FEA), Trochanis et al. (1991) noted that the
95 axial response of a single pile is identical whether the soil is modeled as elastic or elastoplastic
96 when slip is accommodated at the pile-soil interface as shown in Fig. 3 (see Fig. 1(a) for
97 definitions of pile/soil parameters). These authors concluded that soil nonlinearity must
98 therefore be concentrated at the pile-soil interface from which it was deduced that the soil
99 remains in a linear elastic state outside of this narrow region.

100 Leung et al. (2010) investigated the role of linear elasticity in pile group analysis by appraising
101 LE and nonlinear methods for the analysis of pile groups against hypothetical scenarios and
102 published case histories. These authors observed that within a pile group the “*nonlinearity in*
103 *individual pile behavior becomes overwhelmed by the interaction effects*” and therefore pile
104 interaction is governed by elastic behaviour (see Fig. 4).

105 Ju (2015) explored the role of soil stiffness nonlinearity on pile interaction using three-
106 dimensional FEA. Three types of analyses were carried out: (1) a LE analysis of the entire soil
107 domain; (2) a composite LE-nonlinear analysis where the soil immediately surrounding the
108 piles was considered nonlinear and the rest of the soil considered LE; (3) a nonlinear analysis
109 of the entire soil domain. This author noted that the type-2 analysis provided significantly
110 improved agreement to field measurements by comparison to the type-1, which would be
111 expected. Surprisingly, the agreement between FEA predictions and the measured response

112 was poorer for the type–3 compared to the type–2 analysis. It should be noted, however, that
113 this comparison is highly dependent on the equivalent elastic stiffness adopted in the type–2
114 analysis. Nevertheless, these comparisons revealed that soil stiffness nonlinearity is confined
115 to a radial distance of one pile diameter from the pile surface, slightly greater than that implied
116 by Caputo and Viggiani (1984).

117 McCabe and Sheil (2015) employed a constitutive model featuring a stress–dependent
118 nonlinear stiffness to explore the appropriateness of nonlinear IFM for predicting pile group
119 settlement. This was achieved through comparison of settlement predictions determined from
120 (i) a full 3D analysis of the entire group and (ii) superposition of α using both Approach I and
121 Approach II IFM. For floating pile groups, good agreement was observed between the direct
122 and Approach I IFM methods. Comparisons between the direct and Approach II IFM
123 predictions were less satisfactory. An example comparison is provided in Fig. 5 for a rigidly–
124 capped floating pile group with a pile spacing–to–diameter (s/D) ratio of 3 and a load factor
125 (LF) of 0.4 on the capacity of a single pile. Locating a stiffer stratum at the base of the piles
126 was also shown to reduce the accuracy of Approach I predictions, although with a bias on the
127 conservative side.

128 Wang et al. (2016a) presented similar comparisons between IFM and direct FEA. The IFM
129 predictions involved coupling analytical single pile settlement predictions with the elastic
130 interaction factors reported in Poulos and Davis (1980). Predictions of the total interaction
131 experienced by a centre group pile for groups sizes, N , of 9, 25, and 49 piles are shown in Fig.
132 6. These authors suggested that “group reinforcing effects” on the soil continuum have a non–
133 negligible influence on the accuracy of IFM, when compared to FEA, and they proposed a
134 ‘linear approximate method’ to account for group reinforcing effects that demonstrated
135 improved agreement to the direct analyses. Wang et al. (2016b) presented additional numerical
136 results in an effort to reconcile the differences between IFM and FEA. This process involved
137 determining the value of α between a loaded source pile and a non–loaded receiver pile
138 (labelled piles $a - d$) using Approach I within groups of increasing size (see Fig. 7). Figure 8
139 shows that the influence of group reinforcing effects (i.e. the presence of intervening non–
140 loaded group piles) on α appear to be minimal for the group sizes and soil parameters
141 considered in this example.

142

143

144 **EMPIRICAL METHODS**

145 *Overview of existing methods*

146 Empirical approaches allow pile group settlement performance to be determined directly, but
147 based on experience from field/laboratory tests or advanced numerical modelling rather than a
148 theoretical basis. The pile group settlement ratio, R_s , is the most common means of quantifying
149 the extent of pile interaction within a pile group. This factor can be considered as an
150 amplification factor on the settlement of a single pile subjected to an equivalent pile head load:

$$R_s = \frac{w_{group}}{w_{single}} \quad (2)$$

151 where w_{group} and w_{single} are the settlements of a pile group and single pile with the same head
152 load per pile, respectively.

153 Skempton (1953) developed what appears to be the earliest empirical expression for R_s based
154 on field tests of driven pile groups in sand:

$$R_s = \left(\frac{4B' + 2.7}{B' + 3.6} \right)^2 \quad (3)$$

155 where B' is the width of the plan area of the pile group in metres.

156 Meyerhof (1959) included the influence of pile spacing and the number of piles for square pile
157 groups located in sand based on theoretical observations:

$$R_s = \frac{s/D(5 - \frac{(s/D)}{3})}{\left(1 + \frac{1}{n_r}\right)^2} \quad (4)$$

158 where n_r is the number of rows of piles in a square pile group.

159 Vesic (1969) simply related R_s to the pile group width, B_g , normalised by the pile diameter:

$$R_s = \sqrt{\frac{B_g}{D}} \quad (5)$$

160 Kaniraj (1993) developed a semi-empirical equation for R_s . A new term was introduced by this
161 author, termed the 'settlement ratio for equal stress', R'_s , and defined as the ratio of the
162 settlement of a pile group to that of a single pile when the average stress on their respective
163 load transmitting areas are equal:

$$R'_s = 1.128 \sqrt{\frac{(n_r - 1)(n_c - 1)(S/D)^2}{\left(1 + 2\frac{L}{D}\tan\theta\right)^2} + \frac{(n_r + n_c - 2)\left(\frac{S}{D}\right)}{1 + 2\frac{L}{D}\tan\theta}} + 1 \quad (6)$$

164 where θ is the load dispersion angle, taken as $\sim 7^\circ$ according to (Berezantzev et al. 1961), and
 165 n_c is the number of columns of piles in the pile group. The value of R_s may then be determined
 166 as follows:

$$R_s = 1 + 0.67 \left(\frac{N_p S_{sh}}{R'_s S'_{sh}} - 1 \right) \quad (7)$$

167 where S'_{sh} and S_{sh} are the secant slopes of the hypothetical single pile load–displacement curve
 168 under loads of qA_g/N and qA_s respectively and q is the applied stress. The term S'_{sh}/S_{sh} is used
 169 to account for soil nonlinearity.

170 Castelli and Maugeri (2002) developed an approach based on the equivalent pier method
 171 combined with a hyperbolic load–transfer function to model nonlinear interaction with soil:

$$R_s = \left(\frac{D}{D_g} \right)^{-\varepsilon} \quad (8)$$

172 where D_g is the equivalent diameter of the plan area of the pile group, and an exponent of $\varepsilon =$
 173 0.15 was derived from a limited database of pile group case histories.

174 McCabe and Lehane (2006) recast the Castelli and Maugeri (2002) approach to provide
 175 improved agreement to a database of nine published pile group case histories. However, these
 176 authors considered the group stiffness efficiency, η_g , defined as the inverse of R_s :

$$\eta_g = R_s^{-1} = \frac{[D_g/D]^{0.66}}{N} \quad (9)$$

177 Comodromos (2004) developed an approach through curve–fitting to numerically–derived
 178 values of R_s . Three–dimensional finite difference analyses using an elastic–plastic soil model
 179 were adopted for this purpose. The group sizes considered in the parametric analyses ranged
 180 from 4 piles to 25 piles while a spacing of three pile diameters was maintained. Comodromos
 181 and Bareka (2009) presented additional numerical analyses to extend the applicability of their
 182 earlier approach to pile spacings ranging between two and five pile diameters, a broader range
 183 of clayey soils, and alternative group configurations. Their expression is given below:

$$R_s = 0.8[S_{ns}^{0.07}(1.23N_R)^{1.9} + S_{ns}^{-0.08}e^{0.54N_R}] \ln \left(1.25 + \frac{5}{s/D} \right) \quad (10)$$

184 where S_{ns} is the settlement of a single pile, normalised by the pile diameter and N_R is defined
 185 by Comodromos et al. (2016) for large group sizes:

$$N_R = \frac{(N + 5)^{0.85}}{n_r + n_c} \quad (11)$$

186 Sheil and McCabe (2014) developed closed-form equations by curve-fitting results obtained
 187 from 3D FEA using a nonlinear soil model. The influence of pile spacing, length, group
 188 geometry and size, as well as the depth and stiffness of an underlying bearing stratum were all
 189 considered in the parametric analyses. Three sets of equations to predict η_g were developed for
 190 (i) pile groups in infinitely deep soil mass ($h/L \geq 3$), (ii) pile groups in a finite soil mass ($1 <$
 191 $h/L < 3$), and (iii) pile groups end-bearing on a stiff soil stratum ($h/L = 1$), where h is the depth
 192 below ground level to a stiff bearing stratum.

193 For case (i), the following equation was developed where η_f signifies η_g for a floating pile
 194 group:

$$\eta_g = \eta_f = \frac{[D_g/D]^A}{N + 1} \quad (12)$$

195 where $A = 0.83(L/D)^{-0.071}$. To account for the presence of a stiff bearing stratum beneath the
 196 base of the pile group (case (ii)), additional terms were added to equation (12):

$$\eta_g = \eta_f + B \left(\frac{1}{h/L} \right)^6 \quad (13)$$

197 where $B = 0.147(L/D)^{-0.272} \ln N$. Finally, the expression developed for case (iii) was defined as
 198 follows:

$$\eta_g = \eta_f \times \left(\frac{E_2}{E_1} \right)^C \quad (14)$$

199 where E_2/E_1 is the stiffness of the bearing stratum relative to the soil along the pile shaft, and
 200 $C = 0.112 \ln N - 0.11$.

201

202 *Comparison of empirical methods*

203 Predictions of R_s determined by these empirical approaches are compared in Fig. 9 for a
 204 variation in the number of piles (Fig. 9(a)) and pile spacing-to-length ratio (s/L ; Fig. 9(b)). A
 205 selection of comparable field data has also been superimposed on these figures; the relevant

206 particulars are provided in Table 1. From Fig. 9(a), it can be seen that the associated predictions
 207 span a relatively broad spectrum. This highlights the importance of the data used in the
 208 development, calibration, and validation of these models and the corresponding range of
 209 applicability (see Table 2). In particular, the approaches developed by Comodromos (2004)
 210 and Comodromos and Bareka (2009) predict a steep increase in R_s with an increase in pile
 211 numbers. Comodromos et al. (2016) noted, however, that this approach was developed for
 212 smaller pile groups ($N \lesssim 25$) and is likely to over-predict R_s for large groups. It can also be
 213 seen that predictions determined using the Skempton (1953) and Vesic (1969) are overly
 214 conservative, particularly for smaller pile groups. In contrast, predictions determined using the
 215 Castelli and Maugeri (2002) approach plot notably lower. This is due to the large proportion
 216 of end-bearing pile groups in the database of case histories used for calibration.

217 Considering the influence of s/L in Fig. 9(b), the three oldest approaches in this comparison
 218 predict an increase in R_s with increasing s/L predictions (the Meyerhof (1959) predictions
 219 exhibit a turning point at $s/L \approx 0.3$), which contradicts the more recent approaches as well as
 220 the field data. This is probably due to the limited data from which the latter methods were
 221 developed.

222

223 ANALYTICAL METHODS

224 *Overview of existing pile shaft interaction models*

225 The aforementioned research on nonlinear soil behaviour has formed a basis for the use of the
 226 principle of superposition in nonlinear simplified predictive methods. These approaches vary
 227 in the number of parameters required to calibrate soil nonlinearity, their treatment of the elastic
 228 interaction displacements and conditions at the pile–soil interface such as whether slip is
 229 allowed (see Table 2).

230 Caputo and Viggiani (1984) documented one of the earliest nonlinear pile interaction methods.
 231 These authors compiled all values of α that exist with a group into a single interaction matrix.
 232 Off-diagonal entries, α_{ij} ($i \neq j$), were assumed constant (independent of load level), whereas α_{ii}
 233 varied depending on the load level to account for soil nonlinearity:

$$\alpha_{ii} = \frac{1}{1 - \frac{Q_i}{Q_{i,lim}}} \quad (15)$$

234 where α_{ii} is the interaction factor for pile i under its own load, Q_i , and the ultimate load is $Q_{i,\text{lim}}$,
 235 as defined in Chin (1970).

236 Lee (1993) documented a simplified hybrid layer approach for predicting pile interaction; a
 237 hyperbolic relationship between mobilised shear stress and displacement at the pile–soil
 238 interface was used to consider soil stiffness nonlinearity. This author modified the Randolph
 239 and Wroth (1978) elastic model, introducing a new stress–dependent β term. The incremental
 240 soil settlement Δw_s for a single pile is obtained as follows:

$$\Delta w_s = \frac{\Delta P_s}{2\pi G_t L} \left[\ln \left(\frac{r_m - \beta}{r_0 - \beta} \right) + \frac{\beta(r_m - r_0)}{(r_m - \beta)(r_0 - \beta)} \right] \quad (16)$$

$$\beta = \tau_0 r_0 R_f / \tau_f, \quad (17)$$

241 where ΔP_s is the incremental load at the shaft node, G_t is the initial tangent shear modulus at
 242 the pile shaft, L is the pile length, r_0 is the pile radius, r_m is the lateral distance from the pile
 243 centre at which the shear stress is considered negligible (Randolph and Wroth 1978), R_f is a
 244 hyperbolic parameter, and τ_0 and τ_f are the current and limiting shear stress at the pile–soil
 245 interface respectively. For the calculation of α , this author adopted the elastic solutions
 246 documented in Randolph and Wroth (1979):

$$\alpha_{ij} = \frac{\ln \left(\frac{r_m}{r_s} \right)}{\ln \left(\frac{r_m}{r_0} \right)} \quad (18)$$

247 It is important to note that these values of α were applied to the elastic portion of the soil
 248 displacements (which may be obtained by setting the parameter β to zero).

249 As part of the French national project FOREVER, Maleki and Frank (1994) documented the
 250 development of the ‘GOUPEG’ program for the analysis of micropiles installed in groups. This
 251 method was considered a hybrid approach. The analysis of a single pile was conducted using
 252 the load transfer method. Mindlin’s elasticity solutions were used to automatically calculate
 253 the ‘interactive’ displacements induced on adjacent piles. The displacement component of the
 254 single pile t-z curves was then modified to account for these additional interactive
 255 displacements.

256 Costanzo and Lancellotta (1998) developed an analytical solution for nonlinear values of α for
 257 floating rigid piles. These authors proposed a linear variation of shear modulus with radial
 258 distance from the pile to simulate, in a simplified manner, the degradation of shear modulus
 259 due to shear strain:

$$G(r) = G_{min} + \frac{G_{max} - G_{min}}{r_l - r_0} (r - r_0) \quad (19)$$

260 where $G(r)$ is the current shear modulus at a radius r from the pile, G_{max} and G_{min} are the
 261 maximum and minimum shear moduli occurring at a very large distance from the pile axis (r_l ,
 262 taken as $8.0D$) and at the interface of the pile (r_0), respectively. The load–transfer relationship
 263 was subsequently defined as:

$$w_s = \frac{r_0}{G_{min}} \ln\left(\frac{r_l}{r_0}\right) \tau_0 \quad (20)$$

264 The free–field displacement field around a loaded pile (Randolph and Wroth 1979) was used
 265 to superimpose the effects of adjacent piles in the group, again ignoring the receiver pile
 266 reinforcing effect. The interaction between piles may then be determined as follows:

$$\alpha = 1 - \frac{\ln\left(\frac{s}{r_0} \frac{G_{min}}{G(s)}\right)}{\ln\left(\frac{r_l}{r_0} \frac{G_{min}}{G_{max}}\right)} \quad (21)$$

267 The influence of a reduced near–pile modulus on α using this approach is presented in Fig. 10.
 268 Lee and Xiao (2001) adopted a discontinuous displacement function in order to confine plastic
 269 soil behaviour to a thin annulus surrounding a loaded pile (see Fig. 11). Outside of this annulus,
 270 the soil was assumed elastic. The pile settlement may be obtained as follows:

$$w_s = \frac{r_0}{G_0} \ln\left(\frac{r_m}{r_0}\right) \tau_0 + \frac{a\tau_0}{1 - b\tau_0} \quad (22)$$

271 where G_0 is the small–strain (initial) stiffness, and parameters a and b describe the nonlinearity
 272 of the load–transfer curve (see Fig. 12). The first part of this expression represents the elastic
 273 soil displacements and corresponds to the solutions of Randolph and Wroth (1979). The second
 274 part represents the nonlinear portion of the displacements, using a hyperbolic model similar to
 275 that proposed by Duncan and Chang (1970). Pile interaction is determined using the free–field
 276 (elastic) soil displacement according to Randolph and Wroth (1979) and these are applied to
 277 the elastic portion of the settlement in equation (22); predictions of the displacement field
 278 surrounding a loaded single pile are shown in Fig. 13. Pile interaction is calculated by including
 279 the axial rigidity of the receiver pile; the final shear stress mobilisation at the interface is
 280 dependent on the relative pile–soil displacement.

281 Zhang *et al.* (2010) adopted a hyperbolic load–transfer model for the pile shaft:

$$\tau_0 = \begin{cases} \frac{w_s}{c + dw_s}; & w_s \leq w_u \\ \tau_f; & w_s \geq w_u \end{cases} \quad (23)$$

282 where c and d are the hyperbolic model fitting parameters, and w_u is the displacement required
 283 to mobilise τ_f . Although parameters c and d should ideally be calibrated against measured
 284 experimental or field data, they may also be estimated from the following expressions (Zhang
 285 et al. 2010):

$$c = \frac{r_0 \ln\left(\frac{r_m}{r_0}\right)}{G} \quad (24)$$

$$d = \frac{R_f}{\tau_f} \quad (25)$$

286 where G is the shear modulus of the soil around the pile shaft. By contrast, no such guidance
 287 is provided for w_u in the absence of measured field or laboratory data. Pile interactive
 288 displacements were obtained by superimposing elastic free-field soil displacements according
 289 to Randolph and Wroth (1979) as defined in equation (18).

290 Zhang and Zhang (2011) considered interaction between piles with dissimilar lengths. The
 291 elastic solutions of Randolph and Wroth (1979) were adopted to describe the load-transfer
 292 relationship; nonlinearity of the load-displacement behavior of a single pile was included by
 293 imposing a maximum shear stress at the pile-soil interface. Instead of using the free-field
 294 displacement for the determination of the response of the non-loaded receiver pile, these
 295 authors also included the effect of the axial rigidity of the pile:

$$E_p A_p \frac{d^2 w_j(z)}{dz^2} - k_z \Delta w_j = 0 \quad (26)$$

296 where z is the depth below ground level, w_j is the pile displacement at point j , k_z is the soil
 297 Winkler spring stiffness, Δw_j is the relative displacement between pile and soil at interface j of
 298 the non-loaded receiver pile, and E_p and A_p are the Young's modulus and area of the pile
 299 respectively. Wong and Poulos (2005) adopted approximate relationships to transform
 300 interaction factors for piles with identical lengths to those with dissimilar lengths. Modified
 301 versions of these expressions were adopted by Zhang and Zhang (2011):

302 For $L_i > L_j$:

$$\alpha'_{ij} \approx \frac{(\alpha_{ii} + \alpha_{jj})}{f_{1s}} \frac{1}{R_{1s}^K \cdot R_{1s}^L} \quad (27)$$

303 For $L_i < L_j$:

$$\alpha'_{ij} \approx \frac{\alpha_{jj}}{f_{s1}} \frac{1}{R_{s1}^K \cdot R_{s1}^L} \quad (28)$$

304 where L_i and L_j are the lengths of piles i and j respectively, f_{is} and f_{s1} are the correction factors
305 for s/D , pile length difference, and soil modulus distribution, R_{s1}^K and R_{1s}^K are the correction
306 factors for the relative stiffness between the pile and soil, R_{s1}^L and R_{1s}^L are the correction factors
307 for the pile slenderness (L/D). Closed-form expressions for these correction factors are
308 provided in Zhang and Zhang (2011) and Wong and Poulos (2005).

309 Wang *et al.* (2012) used a ‘*BoxLucasI*’ function to represent both the relationship between the
310 shear stress and local nonlinear displacement at the pile–soil interface, ΔS :

$$\tau_0 = \tau_f (1 - e^{-A\Delta S}) \quad (29)$$

311 where A is a model parameter defined as follows:

$$A = \frac{G_0}{r_0 \ln\left(\frac{r_m}{r_0}\right) \tau_f} \quad (30)$$

312 The product of A and τ_f can be considered as the initial stiffness of the curve (see Fig. 14).

313 Based on the work of Lee and Xiao (2001), the total displacement at the pile–soil interface is
314 obtained by adding the nonlinear displacements described by equation (29) (confined to the
315 pile shaft) and elastic displacements determined using the Randolph and Wroth (1979)
316 equations. These authors proposed an iterative process to account for the degradation in
317 stiffness of a concrete pile under compressive loads using the well-documented nonlinear
318 Hognestad model (Hognestad 1951; Hognestad *et al.* 1955). The interaction between piles was
319 based on the free-field (elastic) soil displacements which were determined using Randolph and
320 Wroth (1979).

321 Zhang and Zhang (2012) also adopted the hyperbolic load–transfer model (see equation (23))
322 employed by Zhang *et al.* (2010). These authors introduced a ‘reduction coefficient’, λ , to
323 account for the reinforcing effect in a simplified manner:

$$\lambda = \frac{r_0}{s} \frac{\ln\left(\frac{r_m}{s}\right)}{\ln\left(\frac{r_m}{r_0}\right)} \quad (31)$$

324 The modified interaction factor was therefore defined as:

$$\alpha = \left(\frac{s}{r_0} - 1 \right) \lambda \quad (32)$$

325 The influence of the reinforcing effect according to this simplified approach is shown in Fig.
 326 15 along with predictions determined using the Mylonakis and Gazetas (1998) approach. For
 327 close pile spacings ($s/D < 2$) this model predicts an increase in α when reinforcing effects are
 328 taken into account. The minimum value of s/D that should be adopted is therefore equal to 2.
 329 Curiously, the interaction factor defined by equation (32), which is elastic, is applied to the
 330 total displacements, i.e. no distinction is made between plastic and elastic displacements.

331 Jiu and Huang (2014) proposed a simplified approach to consider the nonlinear behaviour of
 332 axially-loaded pile groups installed in layered soils. The nonlinearity of soil stiffness was
 333 confined to a narrow zone surrounding the soil while the soil medium was considered to be in
 334 a linear elastic state based on the findings of Caputo and Viggiani (1984). The nonlinear load–
 335 displacement behaviour of a single pile was considered using the hyperbolic load–transfer
 336 model proposed by Kraft et al. (1981):

$$w_s = \frac{\tau_0 r_0}{G_0} \ln \left(\frac{r_m/r_0 - R_f \tau_0/\tau_f}{1 - R_f \tau_0/\tau_f} \right) \quad (33)$$

337 Solutions for stresses and displacements in a layered elastic half space developed by Ai et al.
 338 (2002) were adopted to calculate elastic two–pile interactive displacements, while also
 339 accounting for the reinforcing effects of the receiver pile on the soil continuum. The principle
 340 of superposition is adopted to extrapolate to group behaviour. It is also possible to simulate
 341 realistic flexibility by coupling this analytical approach with FEA, making use of Mindlin’s
 342 solution for an elastic plate (Mindlin 1951).

343 Sheil and McCabe (2016a; 2016b; 2017) adopted a nonlinear model for the evolution of soil
 344 shear modulus with mean pressure and shear stress level for the development of nonlinear load–
 345 transfer curves previously documented by Lee and Salgado (1999):

$$G = G_0 \left(1 - f \left(\frac{\tau}{\tau_f} \right)^g \right) \left(\frac{p'}{p'_0} \right)^n \quad (34)$$

346 where G is the current shear modulus, f and g are empirical curve fitting parameters, p' is the
 347 mean effective stress which has a far field value of p'_0 , n is a constant between 0.5 and 1 and
 348 controls the stress dependency of soil stiffness.

349 Zhang et al. (2016) also adopted the load–transfer approach proposed by Lee and Xiao (2001)
 350 where the total settlement at the pile shaft is decoupled into elastic and plastic displacements.

351 Receiver pile reinforcing effects were included by relating the shear stress mobilised on the
352 non-loaded receiver pile to the relative displacement between (i) the displacement field
353 induced by the nearby loaded source pile, and (ii) the displacement of the receiver pile.

354

355 *Pile base interaction model*

356 Although the focus of this paper is a review of pile shaft interaction models, a model for the
357 load-displacement relationship at the pile base must be included to enable comparisons with
358 pile groups subjected to compressive axial loads. To this end, the well-documented base model
359 proposed by Chow (1986) has also been adopted here and coupled with the shaft models
360 described above:

$$w_b = \frac{P_b(1 - \nu_s)}{2DG_b} \frac{1}{\left(1 - \frac{R_{fb}P_b}{P_{bu}}\right)^2} \quad (35)$$

361 where w_b is the pile base settlement; P_b is the pile base load; ν_s is the Poisson's ratio of the soil;
362 G_b is the shear modulus at the pile base; P_{bu} is the limiting base load; and R_{fb} is a parameter
363 that determines the extent of soil nonlinearity. The interaction between pile bases (α_b) was
364 considered using the Randolph and Wroth (1979) approach:

$$\alpha_b = \frac{2r_0}{\pi r} \quad (36)$$

365

366 **COMPARISON OF ANALYTICAL MODELS AGAINST FIELD DATA**

367 *Case I: Single pile and pile group load tests, Belfast, Northern Ireland*

368 A selection of the aforementioned analytical models have been used to predict the behaviour
369 of a tension-loaded single pile and five-pile group case history at Belfast, Northern Ireland
370 (McCabe 2002; McCabe and Lehane 2006). Precast square concrete piles with an equivalent
371 diameter, D_{eq} , of 0.282 m were driven to a depth of 6 m in a soft lightly-overconsolidated
372 estuarine silt deposit. The group piles were arranged in a square quincuncial formation at a
373 spacing-to-diameter (s/D_{eq}) ratio of 2.7. An initial elastic shear modulus, G_0 , of 10 MPa was
374 deduced from seismic cone tests which remained relatively constant over the depth of the piles
375 (McCabe 2002). A value of 20 kPa was measured for the in-situ undrained shear strength, s_u ,
376 (incorporating Bjerrum's correction for plasticity index) using a field shear vane (McCabe and

377 Phillips 2008). An adhesion factor of 0.8 combined with a shaft capacity reduction factor, R_t ,
378 of 0.85 to account for ‘barrelling’ of the pile and a loss of effective stress due to tension loading
379 (De Nicola and Randolph 1993) results in a value of $\tau_f = 13.6$ kPa.

380 The parameter selection for each of the analytical approaches is as follows:

- 381 i. For the Lee et al. (1993) predictions, G_0 was adopted for G_t in equation (16) while the
382 value of r_m was calculated as 11.25 m for undrained conditions (Poisson’s ratio, $\nu = 0.5$)
383 and a constant–stiffness profile. A value of 0.9 was assumed for R_f in all instances.
- 384 ii. For the implementation of their methodology, Costanzo and Lancellotta (1998) adopted a
385 shear strain level of the order of 0.27%; from measured stress–strain curves in triaxial
386 compression (McCabe 2002), this corresponds to values of G_{\min} and G_{\max} of $0.1G_0$ and G_0
387 respectively for use in equations (21) and (22). The value of r_1 was assumed as $8.0D$ (2.3
388 m).
- 389 iii. For the Lee and Xiao (2001) approach, the parameters a and b (equation (22)) were
390 determined as the inverse of the initial shear stiffness at the pile–soil interface (assumed
391 to be equivalent to G_0) and the inverse of τ_f respectively.
- 392 iv. A limiting shear displacement, w_u , of 5 mm was adopted in equation (23) for the Zhang et
393 al. (2010) approach based on common values reported in the literature (Sheil and McCabe
394 2016a). Parameters c and d were determined using equations (24) and (25) respectively.
- 395 v. In the Wang et al. (2012) method, parameter A was determined using equation (30).

396 The analytical predictions are compared to measurements of the single pile load–displacement
397 response, interaction between the centre and corner group piles (for $LF = 0.5$), and group load–
398 displacement response in Figs 16(a) – 16(c) respectively.

399

400 *Case II: Ghent Silos, Belgium*

401 Goossens and Van Impe (1991) documented a case history of 40 cylindrical reinforced concrete
402 silos founded on a 1.2 m thick piled raft. The foundation had a footprint of 34 m by 84 m and
403 comprised 697 driven cast-in-situ reinforced concrete piles. The piles were 13.4 m in length
404 (13 m embedded length), 0.52 m in diameter and had an enlarged 0.8 m diameter base. The
405 piles were located in predominantly ‘loamy or clayey sand’. Goossens and Van Impe (1991)
406 used cone penetration test data to deduce a maximum shaft resistance, τ_{f_of} of ~100 kPa and an
407 ultimate base load, P_{bu} , of 2.77 MN. A small-strain shear modulus of 28.6 MPa recommended
408 by Poulos (1993) was also selected here. A default value of 0.9 was adopted for R_{fb} . Two static

409 pile load tests that were conducted at the site were documented by those authors as well as
410 thirteen years of settlement monitoring along the length of the silos. The fully loaded silos,
411 which imposed a footprint pressure of ~ 300 kPa, transferred a load of ~ 1.3 MN to each pile.
412 The normalised spacing between piles (s/D) was calculated as ~ 3.9 . Given the uniform nature
413 of the loading and the thickness of the raft with respect to its footprint, flexible boundary
414 conditions (i.e. equal pile head loads) were assumed at the pile heads within the foundation.
415 The parameter selection followed the same procedure as the previous case study with the
416 following exceptions:

- 417 i. The value of r_m was calculated as 24.4 m ($\nu = 0.25$).
- 418 ii. In the absence of site-specific data, a default value of $0.25G_0$ was adopted for the Costanzo
419 and Lancellotta (1998) approach. Results using two different values for the parameter r_1
420 are compared in Fig. 17(b): $r_1 = 8.0D$ (recommended in Costanzo and Lancellotta 1998)
421 and $r_1 = r_m = 24.4$ m.

422 The analytical predictions are compared to measurements of the single pile tests and the ‘short-
423 term’ settlement distribution of the silos (i.e. approximately two years after construction) in
424 Figs 17(a) and 17(b) respectively.

425

426 *Case III: Liquid ammonia storage tanks, Thessaloniki, Greece*

427 Badellas et al. (1988), Georgiadis et al. (1989) and Savvaidis (2003) reported a case history of
428 settlement measurements of a 38 m diameter liquid storage tank founded on 112 bored piles, 1
429 m in diameter and 42 m long (40.7 m embedded depth). The concrete raft was 0.8 m thick. The
430 soil profile comprised predominantly silty clay. Undrained shear strengths ranging from 36 kPa
431 to 115 kPa were reported by Georgiadis et al. (1989) while the small strain shear moduli ranged
432 between 33 MPa and 226 MPa. The average normalised spacing for the piles was ~ 3.6 . Flexible
433 boundary conditions were again assumed at the pile heads. Fourteen of the piles were
434 monitored for settlement during a water load test in which the tank was filled with 160 MN of
435 water (~ 1.4 MN per pile). The analytical predictions are compared to measurements of the
436 settlement distribution across the diameter of the tanks in Fig. 18.

437

438

439

441 From Fig. 16(a), it can be seen that the models documented by Lee and Xiao (2001), Zhang et
442 al. (2010), and to a lesser extent Zhang and Zhang (2012), all provide good predictions of the
443 single pile load-displacement response at the Belfast site. While the Lee (1993) method
444 provides a very good estimate of the initial stiffness, the nonlinearity is significantly under-
445 predicted. The least satisfactory predictions are obtained using the Costanzo and Lancellotta
446 (1998) approach; it should be noted, however, that significantly improved agreement could be
447 obtained if G_{\min} in equations (19) and (20) was a function of strain or stress level (see equation
448 (34) for example) rather than simply selecting a constant value. Surprisingly, none of the
449 approaches provide an accurate prediction of the two-pile interaction factor, α , in Fig. 16(c).
450 From Fig. 16(b) the approach documented by Zhang et al. (2010) appears to provide the best
451 agreement to the field data. This may, however, be somewhat fortuitous given that this method
452 over-predicts α .

453 For the Ghent silos case history, all methods appear to provide similar predictions of the load-
454 displacement response for the two single pile load tests in Fig. 17(a). This is probably because
455 these methods are dominated by the response of the enlarged pile base and the same base model
456 has been adopted for each approach. It can be seen from Fig. 17(b) that all approaches capture
457 the shape of the settlement distribution reasonably well thereby justifying the assumption of
458 equal pile head loads. In this instance, the methods documented by Lee (1993), Zhang et al.
459 (2010), and Zhang and Zhang (2012) provide the best agreement to the monitored settlements.
460 Two different sets of parameters were used with the approach documented by Costanzo and
461 Lancellotta (1998) i.e. $r_1 = 8.0D$ and $r_1 = r_m$. The former set of parameters provides relatively
462 poor predictions. However, improved agreement is obtained using the relationship $r_1 = r_m$.

463 For the Thessaloniki storage tanks case history, all approaches provide an excellent description
464 of the shape of the settlement distribution again indicating flexible pile cap behaviour. The
465 method by Zhang and Zhang (2012) provides a very good prediction of the settlement
466 distribution followed by the methods of Lee (1993), Wang et al. (2012) and Zhang et al. (2012).
467 It can also be seen that the method proposed by Costanzo and Lancellotta (1998) using $r_1 = r_m$
468 provides good agreement.

469 From an overview of the results presented in Figs 16 – 18, the following general observations
470 can be made regarding each analytical method:

- 471 • Lee (1993): although this method appears to over-predict the stiffness of the load-
472 displacement response for a single pile, this is likely to be attributable to the use of G_t
473 = G_0 in the present paper; the use of a more realistic tangent modulus will therefore
474 provide improved agreement. For working loads where the level of nonlinearity is
475 reduced, this method provides very good predictions of group response.
- 476 • Costanzo and Lacellotta (1998): this method provides poor predictions of single pile
477 and pile group response if the relationships proposed in that study are adopted. In
478 particular, one of the difficulties with this approach is the selection of the G_{\min}
479 parameter. For the Ghent silos and Thessaloniki storage tanks case histories, an
480 arbitrary relationship of $G_{\min} = 0.25G_0$ was adopted given the lack of detailed site
481 investigation. Refinement of this parameter as well as r_1 would improve the predictions
482 significantly.
- 483 • Lee and Xiao (2001): in general, this method provides a good description of the load-
484 displacement response of both a single pile and pile group while the method of
485 determining and applying the pile interactive displacements is rigorous.
- 486 • Zhang et al. (2010): while this approach provides a good description of the load-
487 displacement response of a single pile, the process of applying elastic interaction factors
488 to the total single pile displacements leads to over-predictions of the settlement of a pile
489 group (albeit slight at working loads).
- 490 • Wang et al. (2012): this method captures the initial stiffness of the load-displacement
491 response for a single pile but struggles to capture the highly nonlinear responses
492 considered in the these case histories. Nevertheless, this method provides good
493 predictions of group response due to a rigorous treatment of pile interaction (i.e.
494 application of interaction factors to elastic components of single pile settlement).
- 495 • Zhang and Zhang (2012): although this approach exhibits an unusual distribution for
496 the pile interaction factor as a function of pile spacing (see Fig. 16(b)), the application
497 of the interaction factor to the elastic component of the single pile settlement is a more
498 robust procedure compared to its predecessor (Zhang et al. 2010). In light of this,
499 predictions using this method consistently showed good agreement to the measured
500 data.

501 It should be noted that the predictions presented herein are heavily dependent on the selected
502 input parameters. Insistence upon high quality input parameters that will capture the behaviour

503 of a single pile is a key step in capturing pile group response. These parameters should reflect
504 the type of pile, pile installation effects and the soil behaviour.

505

506 **CONCLUSIONS**

507 In this paper, a database of simplified models has been collated, for use by foundation
508 specialists, enabling the prediction of the nonlinear pile interaction that occurs within
509 vertically-loaded pile groups. These models were categorised as either empirical or analytical.
510 Recent research on the role of soil stiffness nonlinearity in pile interaction has confirmed that
511 the influence of soil plasticity is confined to a narrow zone of soil surrounding a loaded pile
512 whereas pile interactive displacements remain essentially elastic. This has paved the way for
513 the use of the principle of superposition (i.e. the interaction factor method) within a nonlinear
514 analytical framework. The vast majority (if not all) of existing analytical approaches for
515 predicting nonlinear pile group behaviour are therefore coupled with the interaction factor
516 method.

517 Three published case histories, involving different pile types, group sizes (5, 112, and 697
518 piles) and ground conditions, were considered to appraise predictions determined from a
519 selection of the analytical methods reviewed in the paper. This exercise revealed that
520 non-linear soil behaviour is essential if the highly nonlinear load-displacement response of a
521 small pile group is to be captured accurately. For larger pile groups, the response of the group
522 is dominated by elastic interactions and the contribution of soil-nonlinearity is therefore
523 limited. The merit of including non-linear interaction within a design approach therefore
524 appears to be dependent on the group size under consideration. It is worth noting that when the
525 pile shaft resistance is fully mobilised, the continuous form of the interaction factor methods
526 become less reliable and the use of the above methods at the onset of pile-soil slippage is not
527 recommended. Although the methods explored in this paper provide a more rigorous
528 framework for the analysis of pile group response, accurate assessment of pile / soil input
529 parameters remains one of the key challenges in foundation design.

530 In contrast to analytical approaches, the majority of empirical approaches are not formed from
531 a theoretical basis. Instead, these methods are developed, calibrated, and validated against a
532 selection of case histories or numerical results. These approaches therefore have an implicit
533 range of applicability that is often over-looked. In particular, approaches developed from

534 analyses of smaller pile groups provide overly-conservative predictions of pile interaction for
535 large pile groups.

536

537 NOTATION LIST

α	Two-pile interaction factor
β	Stress-dependent term used in Lee (1993)
ε	Exponent used in Castelli and Maugeri (2002) method
η_f	Stiffness efficiency of a floating pile group
η_g	Stiffness efficiency of a pile group
θ	Load dispersion angle
λ	Pile interaction reduction factor due to receiver pile reinforcing effects
τ_f	Limiting shear stress at pile-soil interface
τ_0	Shear stress at pile-soil interface
A	Nonlinear fitting parameters used in Wang et al. (2012) method
A_p	Area of the pile
a, b	Nonlinear fitting parameters used in Lee and Xiao (2001) method
B'	Pile group width used in Vesic (1969) approach
B_g	Width of the plan area of a pile group in metres used in Skempton (1953) approach
c, d	Nonlinear fitting parameters used in Zhang et al. (2010) method
D	Pile diameter (circular) or width (square)
D_{eq}	Equivalent diameter of a non-circular pile
D_g	Equivalent diameter of the plan area of a pile group
E_p	Young's modulus of the pile
f, g	Nonlinear fitting parameters for soil modulus degradation model (Lee and Salgado 1999)
f_{1s}, f_{s1}	Correction factors for pile spacing, pile length difference, and soil modulus distribution used in Zhang and Zhang (2011) method
G_{max}	Maximum (far-field) soil modulus at a distance r_1 from the pile centre
G_{min}	Minimum shear modulus at the pile-soil interface
$G(r)$	Shear modulus at a distance r from the pile centre
G_t	Initial tangent shear modulus at the pile shaft
G_0	Initial small-strain shear modulus
k_z	Soil Winkler spring stiffness
L	Pile length
LF	Load factor (as a fraction of the capacity of a single pile)

L_i, L_j	Length of pile i, j
N	Pile group size
n	Constant controlling the stress-dependency of soil stiffness
n_c	Number of columns of piles in a pile group
n_r	Number of rows of piles in a pile group
ΔP_s	Incremental shaft load
p'	Current mean effective stress of the soil
p'_0	Far-field (undisturbed) mean effective stress of the soil
q	Applied stress
Q_i	Load applied to pile i
Q_{lim}	Ultimate limit load as defined in Chin (1970)
R_f	Hyperbolic model fitting parameter
R_{s1}^L, R_{1s}^L	Correction factors for pile slenderness used in Zhang and Zhang (2011) method
R_{s1}^K, R_{1s}^K	Correction factors for the relative stiffness between the pile and soil used in Zhang and Zhang (2011) method
r_m	Lateral distance from the pile wall at which the shear stress is considered negligible
R_s	Pile group settlement ratio
R'_s	Pile group settlement ratio for equal stress
R_t	Shaft capacity reduction factor during tensile loading due to pile barrelling and loss of effective stress
r_0	Pile radius
s	Spacing between piles
S_{ng}	Displacement of a pile group normalised by the pile diameter
S_{ns}	Displacement of a single pile normalised by the pile diameter
S'_{sh}, S_{sh}	Secant slopes of a hypothetical single pile load–displacement curve used in Kaniraj (1993) method
s_u	Undrained shear strength of the soil
s_{u0}	Far-field (undisturbed) undrained shear strength of the soil
ΔS	Local nonlinear displacement at pile shaft
w_{group}	Displacement of a pile group
Δw_j	Relative displacement between pile and soil at interface j of the non–loaded receiver pile
Δw_s	Incremental soil settlement at pile–soil interface

w_s	Soil displacement at pile-soil interface
w_{single}	Displacement of a single pile
w_u	Displacement required to mobilise limiting shear stress
z	Depth below ground level

538

539

540 REFERENCES

- 541 Ai, Z. Y., Yue, Z. Q., Tham, L. G., and Yang, M. (2002). "Extended Sneddon and Muki
542 solutions for multilayered elastic materials." *International Journal of Engineering*
543 *Science*, 40(13), 1453-1483.
- 544 Bartolomey, A.A., Yushkov, B.S., Doroshkevitch, N.M., Leshin, G.M., Khanin, R.E.,
545 Kolesnik, G.S. and Mulyukov, E.I., 1981. Pile foundation settlement. In *Proc. Tenth*
546 *Int. Conf. Soil Mech. Found. Engng., Stockholm, Sweden, Rotterdam* (pp. 611-614).
- 547 Badellas, A., Savvaidis, P. and Tsotos, S., 1988. Settlement measurement of a liquid storage
548 tank founded on 112 long bored piles. In *Proceedings of 2nd Inter. Symp. on Field*
549 *Measurements in Geomechanics* (pp. 435-442).
- 550 Berezantzev, V. G., Khristoforov, V. S., and Golubkov, V. N. (1961). "Load bearing capacity
551 and deformation of piled foundations " *Proc 5th Int. Conf. Soil Mech. Found.*
552 *Engrg.* Paris, France, 11-15.
- 553 Brand, E.W., Muktabhant, C., Taechathummarak, A. (1972). "Load tests on small foundations
554 in soft clay". *Proceedings on the Performance of Earth and Earth-Supported*
555 *Structures*, ASCE, 1, 903-928.
- 556 Broms B. (1979). "Negative skin friction." *Proc 6th Asian Regional Conference on Soil*
557 *Mechanics & Foundation Engineering*. Singapore, 41-75.
- 558 Caputo, V., and Viggiani, C. (1984). "Pile foundation analysis: A simple approach to
559 nonlinearity effects." *Riv Ital Geotec*, 18(1), 32-51.
- 560 Castelli, F., and Maugeri, M. (2002). "Simplified nonlinear analysis for settlement prediction
561 of pile groups." *Journal of Geotechnical and Geoenvironmental Engineering, ASCE*,
562 128(1), 76-84.
- 563 Chin, T. K. (1970). "Estimation of the ultimate load of piles from tests not carried to failure."
564 *2nd South East Asian Conference on Soil Mechanics and Foundation Engineering*.
- 565 Chow, Y. K. (1986). "Analysis of vertically loaded pile groups." *Int. J. Numer. Anal. Methods*
566 *Geomech.*, 10, 59-72.
- 567 Comodromos, E. M. (2004). "Response evaluation of axially loaded fixed head pile groups
568 using 3D nonlinear analysis." *Soil Found*, 44(2), 31-39.
- 569 Comodromos, E. M., and Bareka, S. V. (2009). "Response evaluation of axially loaded fixed-
570 head pile groups in clayey soils." *Int. J. Numer. Anal. Methods Geomech.*, 33(17), 1839-
571 1865.
- 572 Comodromos, E.M., Papadopoulou, M.C., and Rentzeperis. I.K., (2009) "Pile foundation
573 analysis and design using experimental data and 3-D numerical analysis", *Comput*
574 *Geotech*, 36(5), 819-836.
- 575 Comodromos, E. M., Papadopoulou, M. C., and Laloui, L. (2016). "Contribution to the design
576 methodologies of piled raft foundations under combined loadings." *Can Geotech J*,
577 53(4), 559-577.
- 578 Constanzo, D., and Lancellotta, R. (1998). "A note on pile interaction factors." *Soils and*
579 *Foundations*, 38(4), 97-136.
- 580 De Nicola, A., and Randolph, M. F. (1993). "Tensile and compressive shaft capacity of piles
581 in sand." *Journal of Geotechnical Engineering*, 119(23), 1952-1973.
- 582 Duncan, J. M., and Chang, C. Y. (1970). "Nonlinear analysis of stress and strain in soils." *J.*
583 *Soil Mech. Found. Div., ASCE*, 96(5), 1629-1653.
- 584 Gens, A., and Nova, R. (1993). "Conceptual bases for a constitutive model for bonded soils and
585 weak rocks." *Proceedings of Geotechnical Engineering of Hard Soils-Soft Rocks*,
586 Rotterdam, 485-494.

587 Georgiadis, M., Ptilakis, K., Tsotsos, S. and Valalas, D. (1989). "Settlement of a liquid storage
588 tank founded on piles." In *Proceedings of the 12th International Conference on Soil*
589 *Mechanics and Foundation Engineering, Rio de Janeiro*, Vol. 2, 1057-1060.

590 Ghalesari, A. T., Barari, A., Amini, P. F., and Ibsen, L. B. (2015). "Development of optimum
591 design from static response of pile-raft interaction." *Journal of Marine Science and*
592 *Technology*, 20(2), 331-343.

593 Goossens, D. and VanImpe, W.F., 1991, May. Long-term settlement of a pile group foundation
594 in sand, overlying a clayey layer. In *Proceedings 10th European Conference on Soil*
595 *Mechanics and Foundation Engineering, Firenze, May*(pp. 26-30).

596 Hognestad, E. (1951). "A study of combined bending and axial load in reinforced concrete
597 members." *Bulletin series no. 399. Engineering Experiment Station, University of*
598 *Illinois, Urbana, III.*

599 Hognestad, E., Hanson, N. W., and McHenry, D. (1955). "Concrete stress distribution in
600 ultimate strength design." *ACI Journal*, 52(4), 455-480.

601 Jiu, Y., and Huang, M. (2014). "A simplified nonlinear method for pile group analysis
602 considering pile cap flexibility." *New Frontiers in Geotechnical Engineering.*
603 *Proceedings of the Geo-Shanghai 2014 International Conference*, A. J. P. ie Han, Shui-
604 Long Shen, Sadik Oztoprak, Jie Huang, ed. Shanghai, China.

605 Ju, J. (2015). "Prediction of the settlement for the vertically loaded pile group using 3D finite
606 element analyses." *Marine Georesources & Geotechnology*, 33(3), 264-271.

607 Kaniraj, S. B. (1993). "A semi-empirical equation for settlement ratio of pile foundations." *Soil*
608 *Found*, 33(2), 82-90.

609 Kausel, E., and Roësset, J. M. (1981). "Stiffness matrices for layered soils." *Bulletin of the*
610 *Seismological Society of America*, 71(6), 1743-1761.

611 Kempfert, H. and Rudolf, M., 2005. Effects of actions due to group effect on the superstructure
612 on pile groups. In *Proceedings of the International Conference on Soil Mechanics and*
613 *Geotechnical Engineering* (Vol. 16, No. 4, p. 2133). AA Balkema Publishers.

614 Koizumi, Y. and Ito, K., 1967. Field tests with regard to pile driving and bearing capacity of
615 piled foundations. *Soils and Foundations*, 7(3), pp.30-53.

616 Kraft, L. M., Ray, R. P., and Kagawa, T. (1981). "Theoretical t-z curves." *Journal of the*
617 *Geotechnical Engineering Division, ASCE*, 107(11), 1543-1561.

618 Kumar, A., Patil, M., and Choudhury, D. (2017). "Soil-structure interaction in a combined pile-
619 raft foundation - a case study." *Proc ICE - Geotech Eng*, 170(2), 117-128.

620 Lee, C. Y. (1993). "Pile group settlement analysis by hybrid layer approach." *ASCE Journal of*
621 *Geotechnical Engineering*, 119(6), 984-997.

622 Lee, J. H., and Salgado, R. (1999). "Determination of pile base resistance in sands." *Journal of*
623 *Geotechnical and Geoenvironmental Engineering, ASCE*, 125(8), 673-683.

624 Lee, K., and Xiao, Z. (2001). "A simplified nonlinear approach for pile group settlement
625 analysis in multilayered soils." *Canadian Geotechnical Journal*, 38(5), 1063-1080.

626 Leung, Y. F., Soga, K., Lehane, B. M., and Klar, A. (2010). "Role of linear elasticity in pile
627 group analysis and load test interpretation." *J. Geotech. Geoenviron. Eng.*, 136(12),
628 1686-1694.

629 Liu, J., Xiao, H. B., Tang, J., Li, Q. S. (2004). "Analysis of load-transfer of single pile in layered
630 soils." *Comp Geotech*. 31:127-35.

631 Maleki, F. and Frank, R. (1993). "Groupes de pieux chargés axialement. " *Project National*
632 *FOREVER, Programme.*

633 Mandolini, A., and Viggiani, C. (1997). "Settlement of piled foundations." *Geotechnique*,
634 47(4), 791-816.

635 McCabe, B. A. (2002). "Experimental Investigations of Driven Pile Group Behaviour in Belfast
636 Soft Clay." PhD thesis, Trinity College, Dublin.

637 McCabe, B. A., and Lehane, B. M. (2006). "Behavior of axially loaded pile groups driven in
638 clayey silt." *J. Geotech. Geoenviron. Eng.*, 132(3), 401-410.

639 McCabe, B.A. and Phillips, D.T. (2008) "Design lessons from full-scale foundation load tests."
640 *Proceedings of the 3rd International Conference on Site Characterization*, Taipei, 615-
641 620.

642 McCabe, B. A., and Sheil, B. B. (2015). "Pile group settlement estimation: suitability of
643 nonlinear interaction factors." *ASCE Int. J. Geomech.*, 15(3), 04014056.

644 Meyerhof, G. G. (1959). "Compaction of sands and bearing capacity of piles." *J. Soil Mech.*
645 *Found. Engng, ASCE*, 85(SM6), 1-30.

646 Mindlin, R. D. (1951). "Influence of rotatory inertia and shear on flexural motions of isotropic,
647 elastic plates." *ASME Journal of Applied Mechanics*, 18, 31-38.

648 Mylonakis, G., and Gazetas, G. (1998). "Settlement and additional internal forces of grouped
649 piles in layered soil." *Geotechnique*, 48(1), 55-72.

650 O'Neill, M. W., Hawkins, R. A., Mahar, L. J. (1982). "Load transfer mechanisms in piles and
651 pile groups." *Journal of the Geotechnical Engineering Division, ASCE*, 108(GT12),
652 1605-1623.

653 Poulos, H. G. (1968). "Analysis of the settlement of pile groups." *Geotechnique*, 18(4), 449-
654 471.

655 Poulos, H.G., 1993. *Settlement prediction for bored pile groups*. University of Sydney, School
656 of Civil and Mining Engineering, Centre for Geotechnical Research.

657 Poulos, H. G. (2006). "Pile group settlement estimation - Research to practice." Shanghai, 1-
658 22.

659 Poulos, H. G., and Davis, E. H. (1980). *Pile foundation analysis and design*, Wiley New York.

660 Rampello, S. (1994) "Observed behaviour of large diameter bored piles in medium to stiff
661 clay." *Proceedings of the Workshop on 'Piled Foundations: Experimental*
662 *Investigations and, Analysis and Design*, Napoli, 407-415.

663 Randolph, M. F., and Wroth, C. P. (1978). "Analysis of deformation of vertically loaded piles."
664 *Journal of the Geotechnical Engineering Division, ASCE*, 104(12), 1465-1488.

665 Randolph, M. F., and Wroth, C. P. (1979). "Analysis of the vertical deformation of pile groups."
666 *Geotechnique*, 29(4), 423-439.

667 Savvaidis, P., 2003. Long term geodetic monitoring of the deformation of a liquid storage tank
668 founded on piles. In *Proceedings, 11th FIG Symposium on Deformation*
669 *Measurements, Santorini, Greece*.

670 Sheil, B. B., and McCabe, B. A. (2014). "A finite element based approach for predictions of
671 rigid pile group stiffness efficiency in clays." *ACTA Geotechnica*, 9, 469-484.

672 Sheil, B. B., and McCabe, B. A. (2016a). "An analytical approach for the prediction of single
673 pile and pile group behaviour in clay." *Comput Geotech*, 75, 145-158.

674 Sheil, B. B., and McCabe, B. A. (2016b). "Reply to discussion by Zhang, Feng, Lie and Zhang
675 on "An analytical approach for the prediction of single pile and pile group behaviour in
676 clay" by Brian B. Sheil and Bryan A. McCabe [Comput. Geotech. 75 (2016) 145-158]."
677 *Comput Geotech*, 80, 349-350.

678 Sheil, B. B., and McCabe, B. A. (2017). "Reply to discussion by Li on "An analytical approach
679 for the prediction of single pile and pile group behaviour in clay" by Brian B. Sheil and
680 Bryan A. McCabe [Comput. Geotech. 75 (2016) 145-158]."
681 Sheil, B. B., McCabe, B. A., Hunt, C. E., and Pestana, J. M. (2015). "A practical approach for
682 the consideration of single pile and pile group installation effects in clay: numerical
683 modelling." *Journal of Geo-engineering Sciences*, 2(3,4), 119-142.

684 Skempton, A. W. (1953). "Discussion: Piles and pile foundations." *Proceedings of the 3rd*
685 *International Conference for Soil Mechanics and Foundation Engineering*.

686 Trochanis, A. M., Bielak, J., and Christiano, P. (1991). "Three-dimensional nonlinear study of
687 piles." *Journal of Geotechnical Engineering*, 117(3), 429-447.

688 Trofimenkov, J., 1977. Panel contribution, Session 2, Behaviour of foundation and
689 structures. *Proc. IX ICSMFE*, pp.370-371.

690 Vesic, A. S. (1969). "Experiments with instrumented pile groups in sand." *Performance of*
691 *Deep Foundations*, ASTM, West Conshohocken, Pa., 177-222.

692 Wang, A. D., Wang, W. D., Huang, M. S., and Wu, J. B. (2016a). "Interaction factor for large
693 pile groups." *Géotechnique Letters*, 6, 58-65.

694 Wang, A. D., Wang, W. D., Huang, M. S., Wu, J. B., Sheil, B. B., and McCabe, B. A. (2016b).
695 "Discussion: Interaction factor for large pile groups." *Géotechnique Letters*, 6, 234-
696 240.

697 Wang, Z., Xie, X., and Wang, J. (2012). "A new nonlinear method for vertical settlement
698 prediction of a single pile and pile groups in layered soils." *Computers and*
699 *Geotechnics*, 45(0), 118-126.

700 Wong, S. C., and Poulos, H. G. (2005). "Approximate pile-to-pile interaction factors between
701 two dissimilar piles." *Computers and Geotechnics*, 32(8), 613-618.

702 Xu, Y., and Zhang, L. M. (2007). "Settlement ratio of pile groups in sandy soils from field load
703 tests." *Journal of Geotechnical and Geoenvironmental Engineering*, 133(8), 1048-
704 1054.

705 Zhang, Q.-Q., Liu, S.-W., Zhang, S.-M., Zhang, J., and Wang, K. (2016). "Simplified non-
706 linear approaches for response of a single pile and pile groups considering progressive
707 deformation of pile–soil system." *Soils and Foundations*, 56(3), 473-484.

708 Zhang, Q.-Q., and Zhang, Z.-M. (2012). "Simplified calculation approach for settlement of
709 single pile and pile groups." *Journal of Computing in Civil Engineering*, 26(6), 750-
710 758.

711 Zhang, Q.-Q., Zhang, Z.-M., and He, J.-Y. (2010). "A simplified approach for settlement
712 analysis of single pile and pile groups considering interaction between identical piles
713 in multilayered soils." *Computers and Geotechnics*, 37, 969-976.

714 Zhang, Q., and Zhang, Z. (2011). "Study on interaction between dissimilar piles in layered
715 soils." *International Journal for Numerical and Analytical Methods in Geomechanics*,
716 35(1), 67-81.

717

Table 1 Particulars of the field data presented in Fig. 9

Reference	Pile type	Soil conditions	N	L/D	s/D
Koizumi & Ito (1967)	Driven	Silty clay	9	18.5	3 5 4
Brand et al. (1972)	Driven	Soft sensitive marine clay	4	40	3 2.5 2
Trofimenkov (1977)	Driven	Stiff silty clay	9	30	3.4
Bartolomey et al. (1981)	Driven	Stiff clay	9	39	3
O'Neill et al. (1982)	Driven	Stiff clay	9	48.5	3
Rampello (1994)	Bored	Medium – stiff clays	74	47	3.1
Randolph & Clancy (1994)	Bored	Hard silty clay & dense sand	38	25	3.5

Table 2 Database of empirical approaches and their range of applicability

Reference	Development	Validation data							
		Data	Soil conditions	Installation	Pile type	Load level Single pile capacity	N range	s/D range	L/D range
Skempton (1953)	Field tests	Field tests	Sand	Driven	–	–	–	–	–
Meyerhof (1959)	Theoretical observations	Field tests	–	–	–	–	–	–	–
Vesic (1969)	Field tests	Field tests	Medium sand	Jacked	Aluminium pipe	–	4 – 9	2 – 6	15
Kaniraj (1993)	Theoretical observations from Berezantzev et al. (1961) modified to fit a database of field tests	Field tests	Sand	–	–	0 – 1 (can account for nonlinear behaviour)	–	–	–
Castelli & Maugeri (2002)	Hyperbolic equivalent pier approach	Field tests	Clay, medium sand	Driven	Steel closed-ended pipe, concrete-filled steel pipe	–	4 – 140	3	33 – 44
Comodromos (2004)	3D elastic-plastic FEA	3D elastic-plastic FEA	Soft clay	Bored	Concrete	0 – 1	4 – 25	3	30
Comodromos & Bareka (2009)	3D elastic-plastic FEA	3D elastic-plastic FEA	Soft clay – stiff clay	Bored	Concrete	0 – 1	6 – 25	2 – 5	25 – 50
McCabe & Lehane (2006)	Modified Castelli & Maugeri (2002) hyperbolic approach	Field tests	Soft clay – medium sand	Driven	Concrete, steel pipe	0.4	4 – 97	2.5 – 7.1	18.5 – 26
Sheil & McCabe (2015)	3D nonlinear FEA	Field tests	Clays & sands	Driven, bored	Concrete, steel pipe, timber	0.4	4 – 697	1.8 – 7.1	14 – 107

Table 3 Database of closed-form analytical models for predicting pile interaction and their main features

Reference	Calibration of shaft load-transfer model parameters	Soil stiffness nonlinearity	Pile interaction	Pile-soil slip
Caputo & Viggiani (1984)	Q_{lim} determined using Chin (1970) solutions	Nonlinear expression for α_{ii}	Use of previously-documented elastic interaction factors.	Not included.
Lee (1993)	R_f may be calibrated against measured load-transfer curves or assumed as 0.9; r_m is determined using Randolph & Wroth (1979) expressions.	Hyperbolic load-transfer model.	α determined from elastic free-field soil displacements (Randolph & Wroth 1979) solutions, applied to the elastic component of the source pile displacements.	Redistribution of stresses once pile-soil limiting resistance is reached
Costanzo & Lancellotta (1998)	G_{min} must be determined based on current shear stress level from measured stress-strain curves; r_1 may be determined from FEA or assumed as eight times the pile diameter.	Lateral variation in shear modulus.	α determined from elastic free-field soil displacements (Randolph & Wroth 1979) solutions, applied to total source pile displacements.	Not included.
Lee & Xiao (2001)	Parameters a and b are calibrated against elemental tests of the interface or measured load-transfer curves. Alternatively a may be assumed as the reciprocal of the soil shear stiffness and b the reciprocal of the limiting shear stress. Parameter r_m determined using Randolph & Wroth (1979) expressions.	Hyperbolic model for the nonlinear portion of the load-transfer.	α determined from elastic free-field soil displacements (Randolph & Wroth 1979) solutions, applied to the elastic component of the source pile displacements. Influence of receiver pile rigidity considered by imposing negative skin friction on loaded pile.	Although pile and soil are considered 'noncompatible', full pile-soil slip not possible due to the decoupling of elastic and plastic displacements.
Zhang et al. (2010)	Parameters c , d , R_f and w_{is} are determined experimentally or by back-analysis of field load tests results; a 'simple' analytical approach is also available for the estimation of parameters c and d .	Hyperbolic load-transfer model.	α determined from elastic free-field soil displacements (Randolph & Wroth 1979) solutions, applied to total source pile displacements.	Maximum shear stress enforced at interface introduces pile-soil slip implicitly.
Zhang & Zhang (2011)	Parameter r_m determined using Randolph & Wroth (1979) expressions.	Maximum shear stress imposed at interface.	α determined from elastic free-field soil displacements (Randolph & Wroth 1979) solutions, applied to total source pile displacements. Influence of receiver pile rigidity considered by relating relative settlement to soil spring stiffness.	Maximum shear stress enforced at interface introduces pile-soil slip implicitly.
Wang et al. (2012)	Parameter A is calibrated against elemental tests of the interface or measured load-transfer curves; r_m determined using Randolph & Wroth (1979) expressions; R_f may be calibrated against measured load-transfer curves or assumed as 0.9.	BoxLucas1 function used to define load-transfer curve.	α determined from elastic free-field soil displacements (Randolph & Wroth 1979) solutions, applied to the elastic component of the source pile displacements.	Full pile-soil slip not possible due to the decoupling of elastic and plastic displacements.
Zhang & Zhang (2012)	See calibration for Zhang et al. (2010).	Hyperbolic load-transfer model.	α determined from elastic free-field soil displacements (Randolph & Wroth 1979) solutions, applied to the total displacements of the source pile. Simplified model developed for including pile reinforcing effects.	Maximum shear stress enforced at interface introduces pile-soil slip implicitly.
Jiu & Huang (2014)	Parameter r_m determined using Randolph & Wroth (1979) expressions; R_f may be calibrated against measured load-transfer curves or assumed as 0.9.	Hyperbolic load-transfer model.	Interactive displacements determined using elastic solutions documented by Ai et al. (2002) which also consider receiver pile reinforcing effects.	Not included.
Zhang et al. (2016)	See calibration for Lee and Xiao (2001)	Hyperbolic model for the nonlinear portion of the load-transfer.	α determined from elastic free-field soil displacements (Randolph & Wroth 1979) solutions, applied to the elastic component of the source pile displacements. Influence of receiver pile rigidity considered by imposing negative skin friction on loaded pile.	Full pile-soil slip not possible due to the decoupling of elastic and plastic displacements.

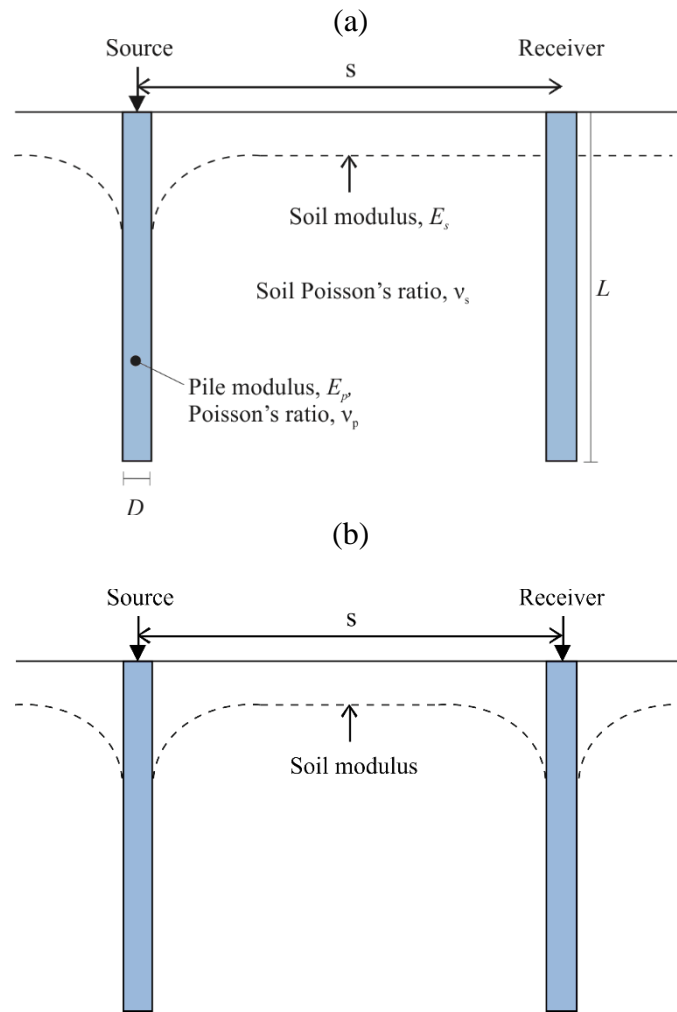


Fig. 1 Illustration of (a) Approach I and (b) Approach II interaction factors

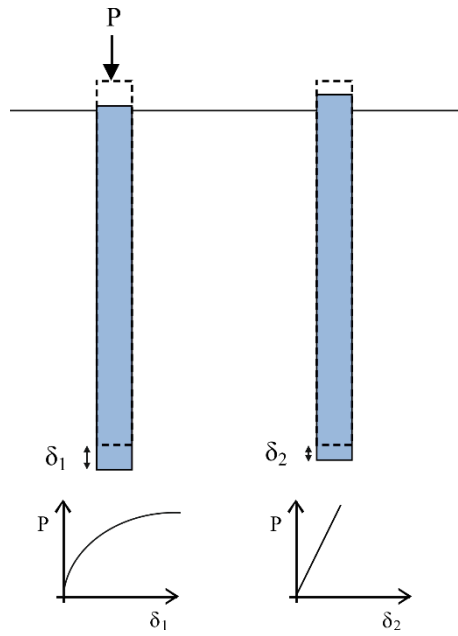


Fig. 2 Illustration of case history and findings documented by Caputo and Viggiani (1984)

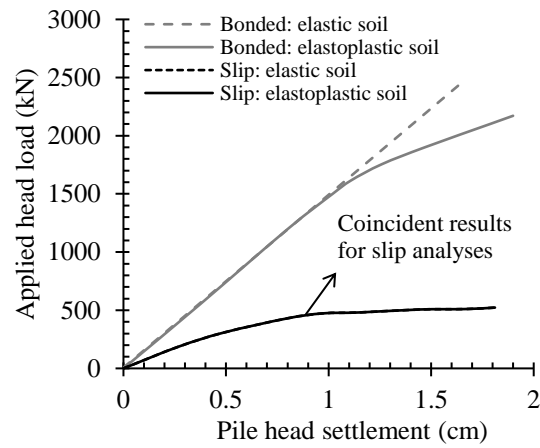


Fig. 3 Influence of slip on the response of a single vertically loaded pile using FEA coupled with an elastic and elastoplastic (Drucker-Prager) model (after Trochanis et al. 1991); $E_p = 20$ GPa, $\nu_p = 0.3$, $L = 10$ m, $B = 0.5$ m, $E_s = 20$ MPa, $\nu_s = 0.45$. Drucker-Prager parameters: $\phi' = 16.7^\circ$, $s_u = 34$ kPa.

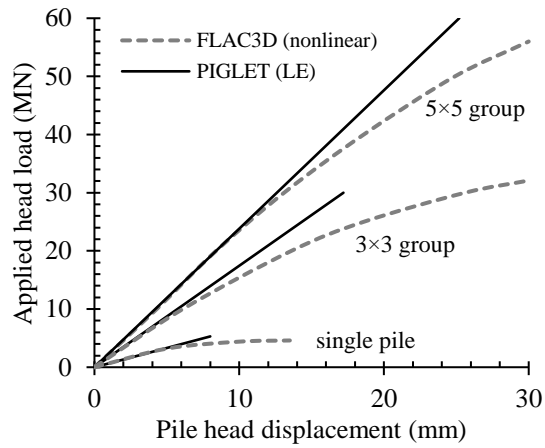


Fig. 4 Comparison of nonlinear and LE numerical analyses (after Leung *et al.* 2010); no interface elements, pile groups connected to rigid cap, $E_p = 30$ GPa, $L = 20$ m, $D = 1$ m, $s = 3$ m, $E_s = 30$ MPa, $s_u = 60$ kPa, $\nu_s = 0.3$

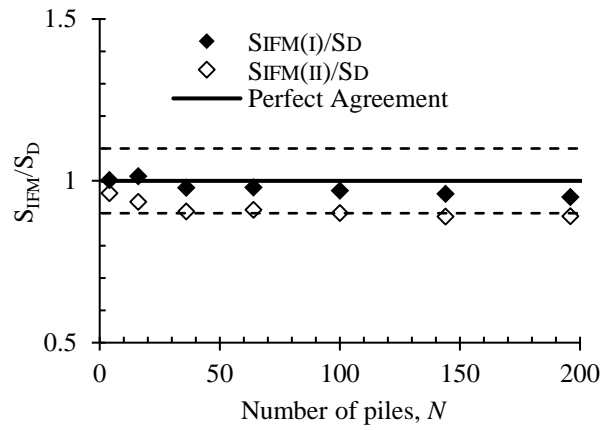


Fig. 5 Comparison between Approach I IFM ($S_{IFM(I)}$), Approach II IFM ($S_{IFM(II)}$), and direct nonlinear (S_D) predictions after McCabe and Sheil (2015); Nonlinear, $L/D = 25$, $s/D = 3$, rigidly-capped floating pile group

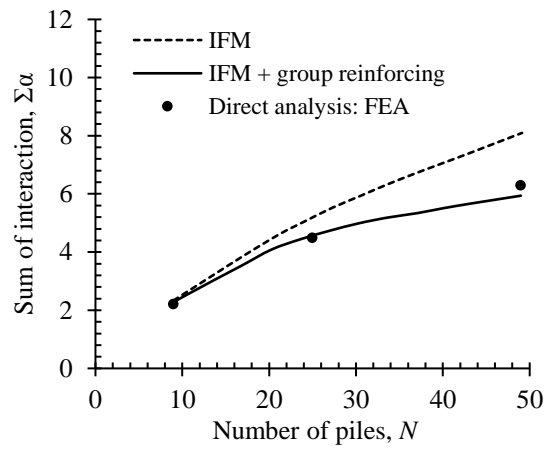


Fig. 6 Comparison of FEA and IFM predictions of the total interaction experienced by a centre group pile; LE, $L = 40$ m, $E_s = 24.5$ MPa, $E_p = 19600$ MPa, $s = 4$ m, $D = 1$ m, $\nu_p = 0.25$, $\nu_s = 0.45$

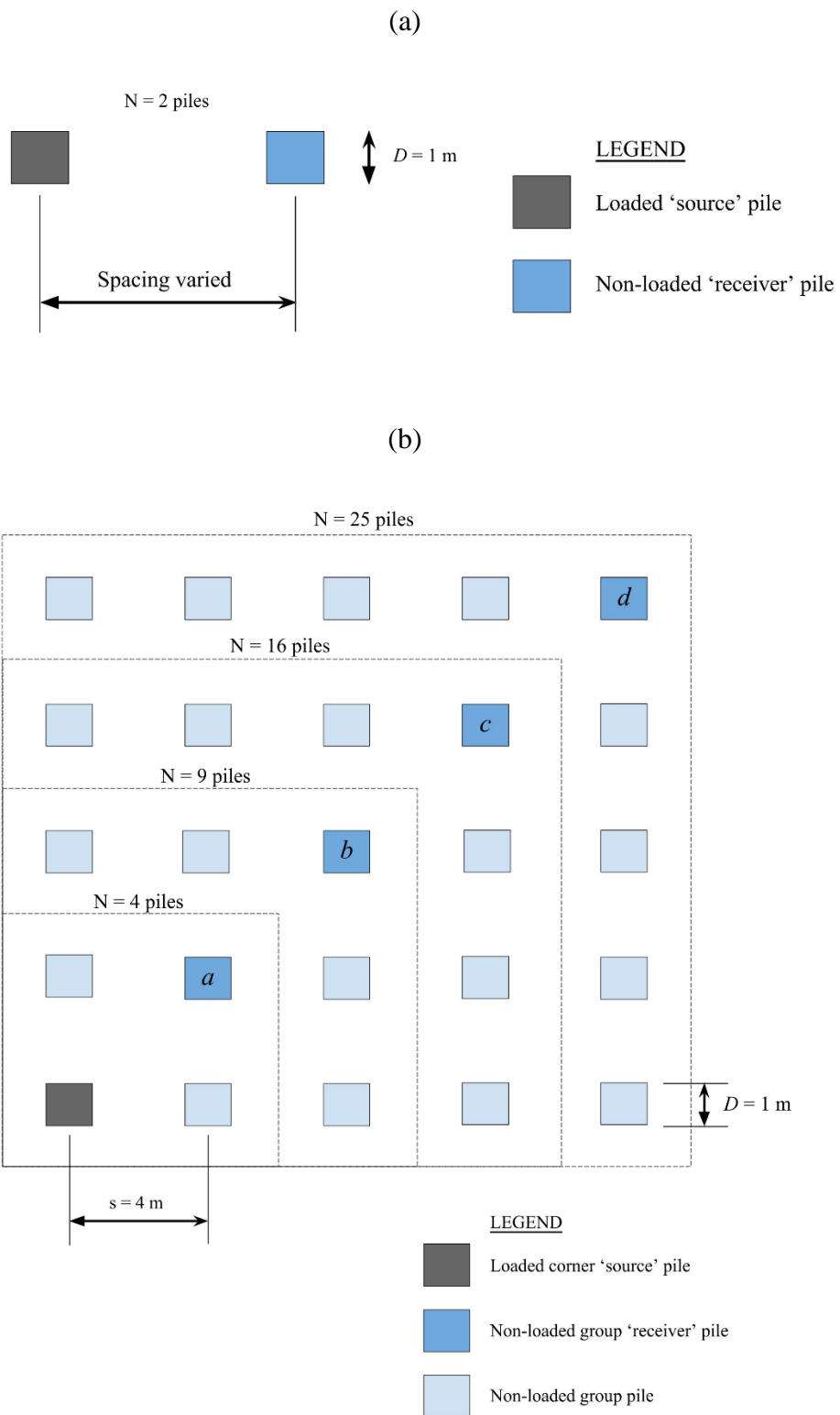


Fig. 7 Illustration of (a) two-pile and (b) pile group geometry (only groups of up to $N = 25$ piles shown for clarity)

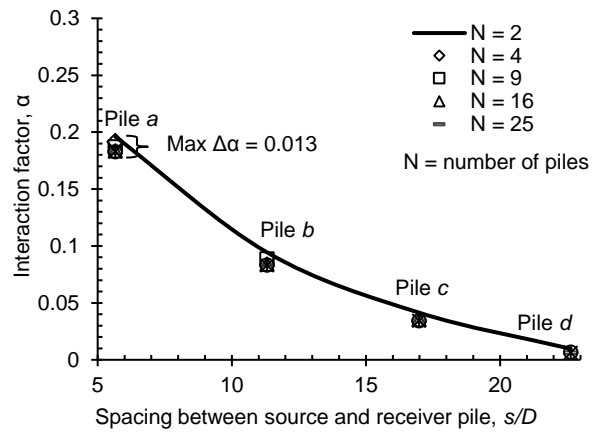


Fig. 8 Influence of intervening free-headed (non-loaded) group piles on two-pile interaction factor using Approach I; $L = 40$ m, $E_s = 24.5$ MPa, $E_p = 19600$ MPa, $s = 4$ m, $D = 1$ m, $\nu_p = 0.25$, $\nu_s = 0.45$

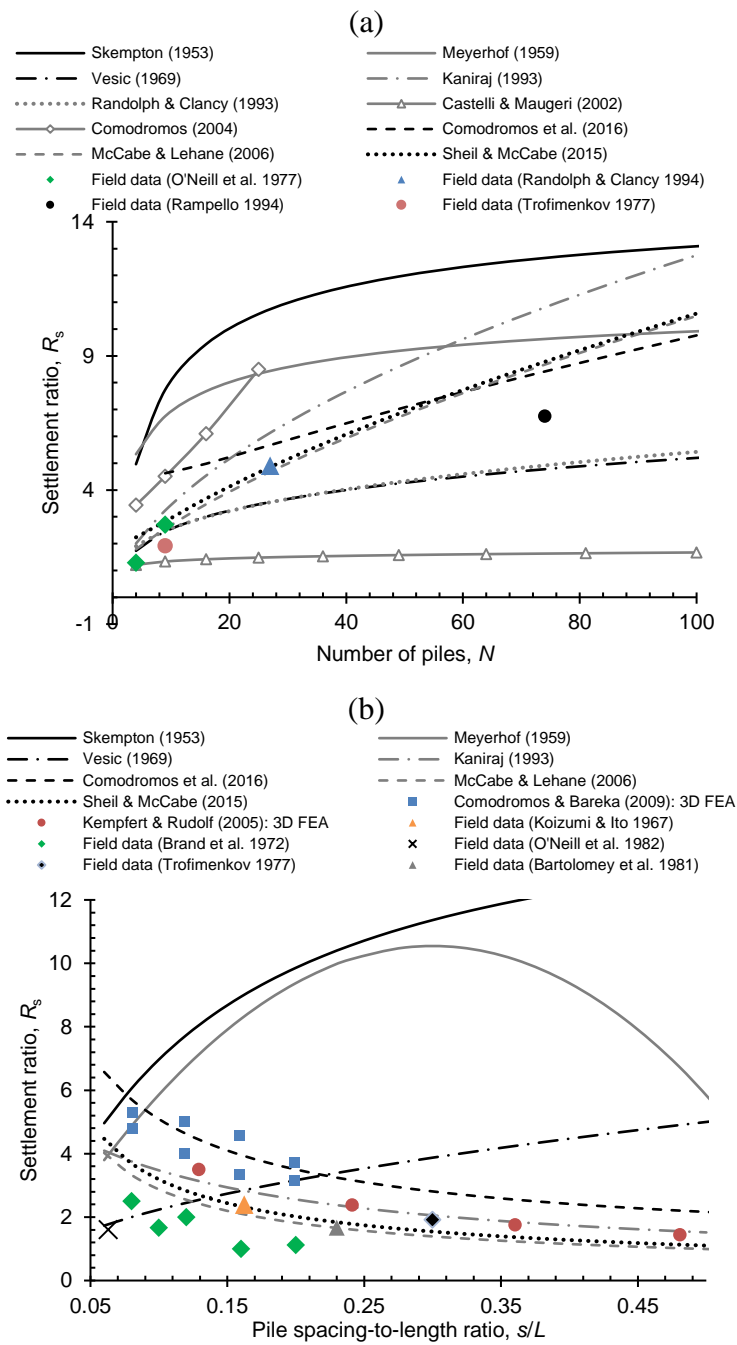


Fig. 9 Comparison of settlement ratio predictions determined using existing empirical approaches: influence of (a) number of piles with common spacing $s = 3.0 D$ ($L/D = 25$), (b) pile spacing-to-length ratio for a 3×3 group layout ($L/D = 25$)

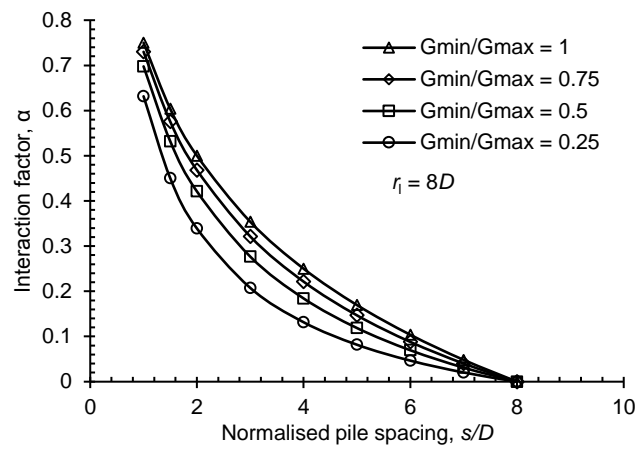


Fig. 10 Influence of reduced 'near-pile' modulus on α (after Costanzo and Lancellotta 1998)

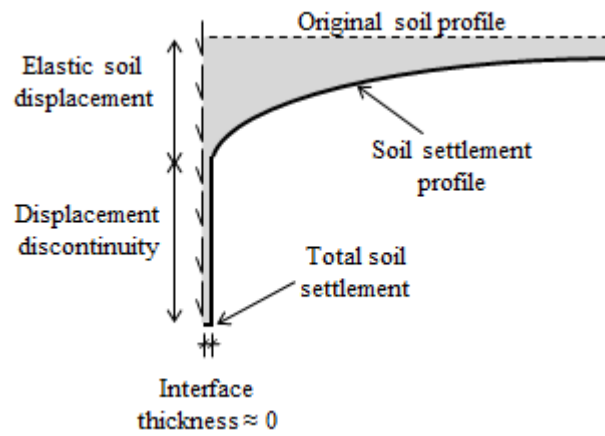


Fig. 11 Illustration of displacement discontinuity concept adopted by Lee and Xiao (2001)

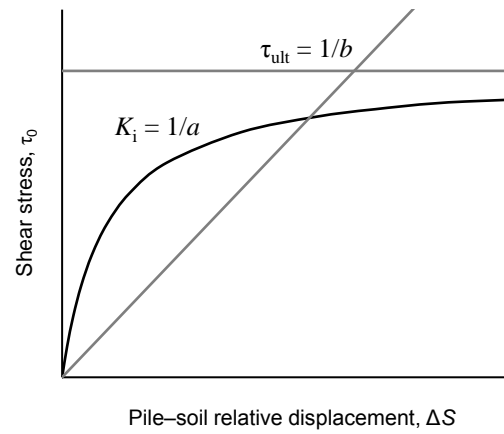


Fig. 12 Hyperbolic relationship between shear stress and relative displacement at pile-soil interface adopted by Lee and Xiao (2001)

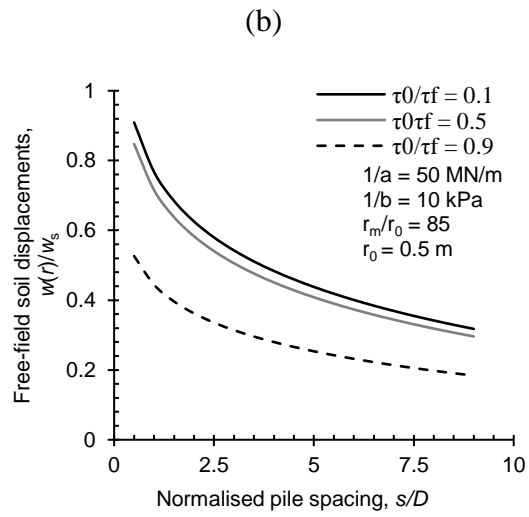
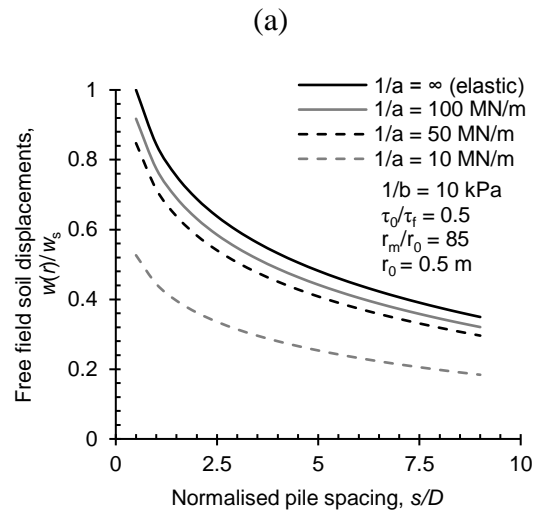


Fig. 13 Normalised free-field soil displacements surrounding a loaded single pile (after Lee and Xiao 2001): (a) influence of parameter a , (b) influence of load level

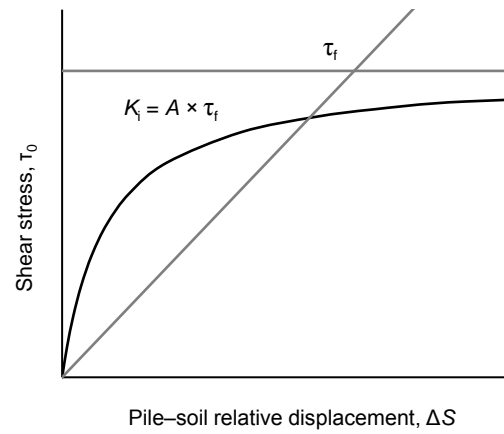


Fig. 14 BoxLucas1 relationship between shear stress and relative displacement at pile-soil interface adopted by Wang et al. (2012)

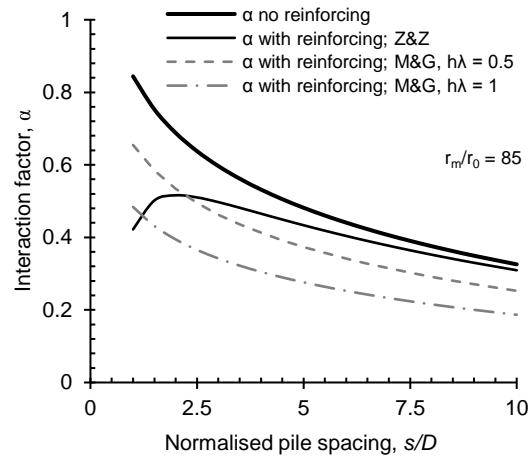


Fig. 15 Comparison of Zhang and Zhang (2012; ‘Z&Z’) simplified model for receiver pile reinforcing effects to that proposed by Mylonakis and Gazetas (1998, ‘M&G’)

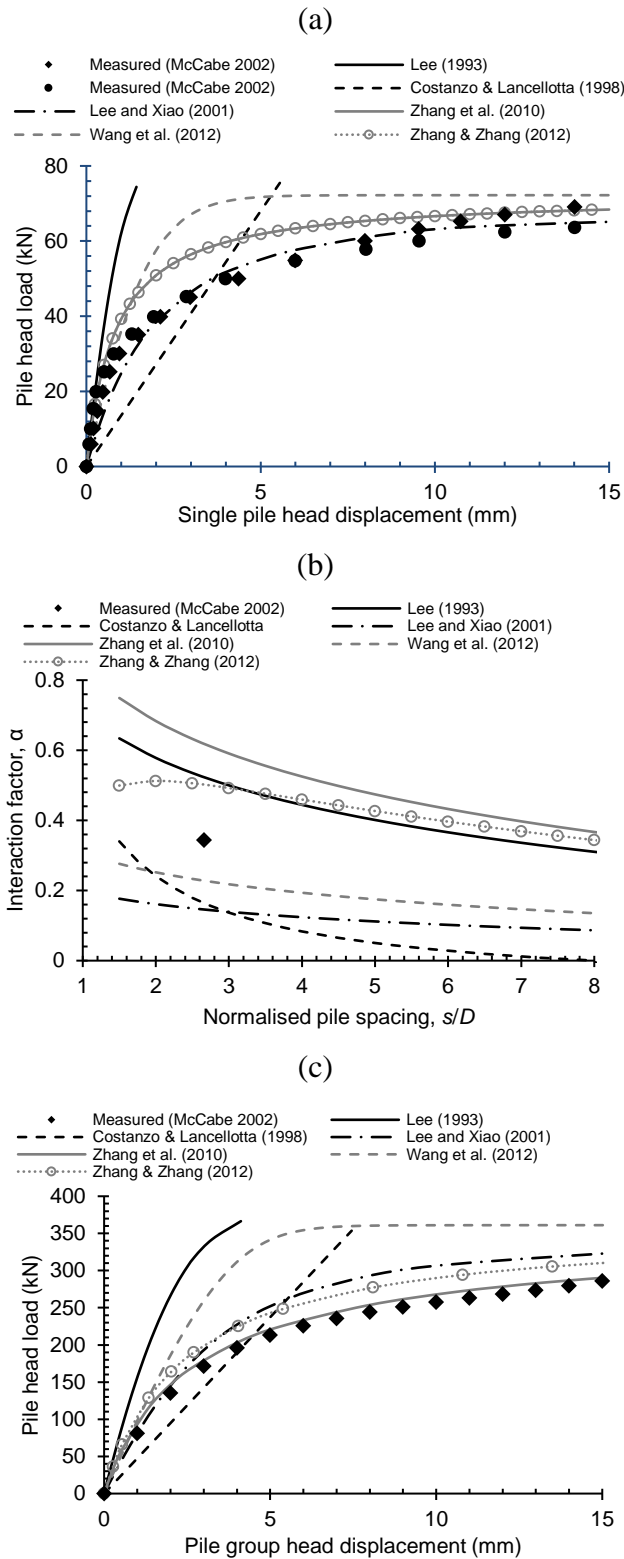


Fig. 16 Comparison of selected analytical approaches to Belfast case history: (a) single pile load-displacement response, (b) two-pile interaction factors (load factor = 0.5), (c) five-pile group load-displacement response; tension loading

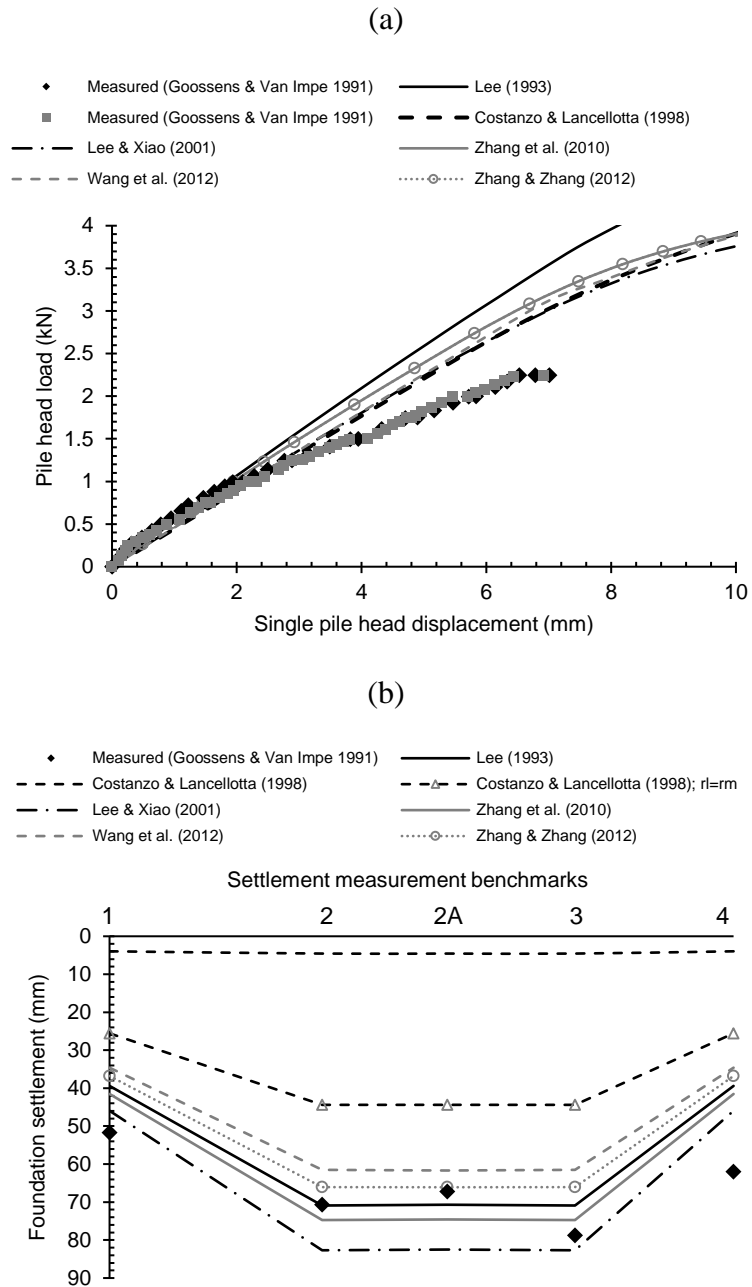


Fig. 17 Comparison of selected analytical approaches to Ghent silos case history: (a) single pile load test, (b) tank settlement distribution across the length of the foundation two years after construction

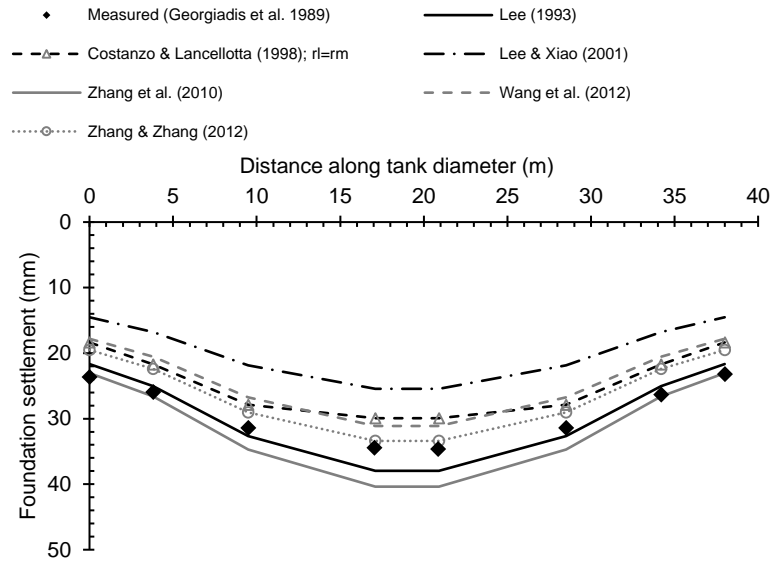


Fig. 18 Comparison of selected analytical approaches to Thessaloniki storage tanks case history: settlement distribution across diameter of foundation